Complex Number RS Coded OFDM with Systematic Noise in the Guard Interval

Mario Huemer*, *Senior Member, IEEE*, Christian Hofbauer*, Johannes B. Huber†, *Fellow, IEEE*
* Klagenfurt University, Institute of Networked and Embedded Systems
Universitaetsstr. 65-67, A-9020 Klagenfurt, {mario.huemer, chris.hofbauer}@uni-klu.ac.at

† University of Erlangen-Nuremberg, Institute for Information Transmission
Cauerstr. 7, D-91058 Erlangen, huber@lnt.de

***Abstract*—Recently we presented a novel OFDM (orthogonal frequency division multiplexing) signaling concept, where the cyclic prefixes (CPs) are replaced by deterministic sequences which we call unique words (UWs). The UWs are generated by appropriately loading so-called redundant subcarriers. By that a complex number Reed Solomon (RS) code construction is introduced which can advantageously be exploited in an LMMSE (linear minimum mean square error) receiver. The overall concept clearly outperforms CP-OFDM in frequency selective channels. In this paper we introduce a method that significantly reduces the energy of the redundant subcarrier symbols by allowing some systematic noise in the UWs. The concept features a notable performance and bandwidth efficiency gain compared to our original UW-OFDM approach.**

I. Introduction

In [1], [2] we introduced an OFDM signaling scheme, where the usual cyclic prefixes are replaced by deterministic sequences, that we call unique words. Fig. 1 compares CP- and UW-based OFDM transmit data structures.

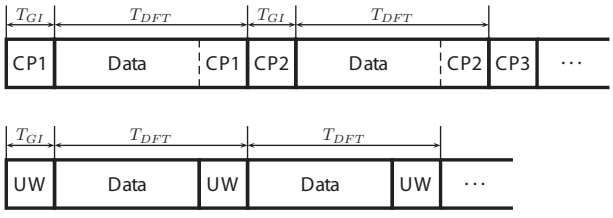

Fig. 1. Transmit data structure using CPs (above) or UWs (below).

In both schemes the linear convolution of the transmit signal with the channel impulse response is transformed into a cyclic convolution. However, there are some fundamental differences between the CP-based and the UW-based approach:

- Different to the CP, the UW is part of the DFT (discrete Fourier transform)-interval as indicated in Fig. 1.
- The CP is a random sequence, whereas the UW is deterministic. Thus, the UW can optimally be designed for particular needs like synchronization and/or channel estimation purposes at the receiver side.

Christian Hofbauer has been funded by the European Regional Development Fund and the Carinthian Economic Promotion Fund (KWF) under grant 20214/15935/23108.

A comparable idea of how to use UWs in OFDM has already been proposed in [3], where the concept is called DMT-KSP (discrete multi-tone - known symbol padding). However, the concept in [3] generates completely different OFDM symbols compared to our approach in [1], and it has to deal with extremely high symbol energies and with the fact, that the performance depends on the particular shape of the UW. Several other attempts of applying UWs in OFDM systems can be found in the literature, e.g. in [4]-[7]. Although named differently like KSP-OFDM, TDS-OFDM (time-domain synchronous OFDM) or PRP-OFDM (pseudorandom postfix OFDM), all concepts share one common property making them completely different from the one in [3] and also from our approach: In all cases, the guard interval and thus the UW is not part of the DFT-interval. Therefore, in contrast to our UW-OFDM approach described below, no coding is introduced by these concepts.

In [1], [2] we suggested to generate UW-OFDM symbols by appropriately loading so-called redundant subcarriers. The minimization of the energy contribution of the redundant subcarriers turned out to be a challenge. We solved the problem by generating a zero UW in a first step and by adding the desired UW in a separate second step. It turned out that this approach generates OFDM symbols with much less redundant energy than a single step or direct UW generation approach. Additionally we optimized the positions of the redundant subcarriers to further reduce their energy contribution. In Sec. II we briefly review our original UW-OFDM concept including the signal generation and the LMMSE data estimation. In Sec. III we show how the redundant subcarrier energy can further be decreased by allowing some systematic noise in the guard interval. With the help of BER (bit error ratio) performance simulations (Sec. IV) we highlight the advantageous properties of the proposed scheme.

Notation: Lower-case bold face variables ($\mathbf{a}, \mathbf{b}$,...) indicate vectors, and upper-case bold face variables ($\mathbf{A}, \mathbf{B}$,...) indicate matrices. To distinguish between time and frequency domain variables, we use a tilde to express frequency domain vectors and matrices ($\tilde{\mathbf{a}}$, $\tilde{\mathbf{A}}$,...), respectively. We further use $\mathbb{C}$ to denote the set of complex numbers, $\mathbf{I}$ to denote the identity matrix, and $(\cdot)^H$ to denote conjugate transposition.

II. Review of UW-OFDM

We briefly review our approach of introducing unique words in OFDM time domain symbols, for further details see [1], [2]. Let $\mathbf{x}_u \in \mathbb{C}^{N_u \times 1}$ be a predefined sequence which we call unique word. This unique word shall form the tail of the OFDM time domain symbol vector. Hence, the time domain symbol vector consists of two parts and is of the form $\begin{bmatrix}\mathbf{x}_d^T & \mathbf{x}_u^T\end{bmatrix}^T$, whereat only $\mathbf{x}_d \in \mathbb{C}^{(N-N_u)\times 1}$ is random and affected by the data. In the concept suggested in [1], [2] we generate an OFDM symbol $\mathbf{x} = \begin{bmatrix}\mathbf{x}_d^T & \mathbf{0}^T\end{bmatrix}^T$ with a zero UW in a first step, and we determine the transmit symbol $\mathbf{x}' = \mathbf{x} + \begin{bmatrix}\mathbf{0}^T & \mathbf{x}_u^T\end{bmatrix}^T$ by adding the UW in time domain in a second step. The latter is trivial, we therefore concentrate on the first step: As in conventional OFDM, the QAM data symbols and the zero subcarriers are specified in frequency domain in vector $\tilde{\mathbf{x}}$, but here in addition the zero-word is specified in time domain as part of the vector $\mathbf{x}$. As a consequence, the linear system of equations $\mathbf{x} = \mathbf{F}_N^{-1}\tilde{\mathbf{x}}$ ($\mathbf{F}_N$ is the DFT matrix) can only be fulfilled by reducing the number N_d of data subcarriers, and by introducing a set of redundant subcarriers instead. We let the redundant subcarriers form the vector $\tilde{\mathbf{r}} \in \mathbb{C}^{N_r \times 1}$ with $N_r = N_u$, further introduce a permutation matrix $\mathbf{P} \in \mathbb{C}^{(N_d+N_r)\times(N_d+N_r)}$, and form an OFDM symbol (containing $N - N_d - N_r$ zero subcarriers) in frequency domain by

$$\tilde{\mathbf{x}} = \mathbf{B}\mathbf{P}\begin{bmatrix}\tilde{\mathbf{d}}\\ \tilde{\mathbf{r}}\end{bmatrix}. \tag{1}$$

$\mathbf{B} \in \mathbb{C}^{N\times(N_d+N_r)}$ is a trivial matrix and inserts the usual zero subcarriers. We will detail the reason for the introduction of the permutation matrix $\mathbf{P}$ and its specific construction shortly below. The time - frequency relation of the OFDM symbol can now be written as

$$\mathbf{F}_N^{-1}\mathbf{B}\mathbf{P}\begin{bmatrix}\tilde{\mathbf{d}}\\ \tilde{\mathbf{r}}\end{bmatrix} = \begin{bmatrix}\mathbf{x}_d\\ \mathbf{0}\end{bmatrix}. \tag{2}$$

With

$$\mathbf{M} = \mathbf{F}_N^{-1}\mathbf{B}\mathbf{P} = \begin{bmatrix}\mathbf{M}_{11} & \mathbf{M}_{12}\\ \mathbf{M}_{21} & \mathbf{M}_{22}\end{bmatrix}, \tag{3}$$

where $\mathbf{M}_{ij}$ are appropriate sized sub-matrices, it follows that $\mathbf{M}_{21}\tilde{\mathbf{d}} + \mathbf{M}_{22}\tilde{\mathbf{r}} = \mathbf{0}$, and hence $\tilde{\mathbf{r}} = -\mathbf{M}_{22}^{-1}\mathbf{M}_{21}\tilde{\mathbf{d}}$. With the matrix

$$\mathbf{T} = -\mathbf{M}_{22}^{-1}\mathbf{M}_{21} \tag{4}$$

($\mathbf{T} \in \mathbb{C}^{N_r\times N_d}$), the vector of redundant subcarriers can thus be determined by the linear mapping

$$\tilde{\mathbf{r}} = \mathbf{T}\tilde{\mathbf{d}}. \tag{5}$$

Equation (5) introduces correlations in the vector $\tilde{\mathbf{x}}$ of frequency domain samples of an OFDM symbol. The construction of $\mathbf{T}$, and thus also the variances of the redundant subcarrier symbols, highly depend on the choice of $\mathbf{P}$. We found that the mean energy of the redundant subcarrier symbols almost explodes without the use of the permutation matrix, or equivalently for $\mathbf{P} = \mathbf{I}$. In [1] we showed that the selection

$$\mathbf{P} = \operatorname{argmin}\left\{\operatorname{tr}(\mathbf{T}\mathbf{T}^H)\right\}, \tag{6}$$

where $\mathbf{T}$ is derived from (3) and (4), provides minimum energy on the redundant subcarriers on average (when averaging over all possible data vectors $\tilde{\mathbf{d}}$). We will graphically illustrate the (optimum) power distribution over all subcarrier symbols for a specific system setup later in Fig. 2.

Throughout this paper we will compare different UW-OFDM approaches with the classical CP-OFDM concept. The IEEE 802.11a WLAN standard [8] serves as reference system. We apply the same parameters for UW-OFDM as in [8] wherever possible, the most important parameters are specified in Table I.

TABLE I
Main PHY parameters of the investigated systems.

	802.11a	UW-OFDM
Modulation schemes	BPSK, QPSK, 16QAM, 64QAM	BPSK, QPSK, 16QAM, 64QAM
Coding rates (outer code)	1/2, 2/3, 3/4	1/2, 2/3, 3/4
Occupied subcarriers	52	52
Data subcarriers	48	36
Additional subcarriers	4 (pilots)	16 (redundant)
DFT period	3.2 μs	3.2 μs
Guard duration	800 ns (CP)	800 ns (UW)
Total OFDM symbol duration	4 μs	3.2 μs
Subcarrier spacing	312.5 kHz	312.5 kHz

The sampling frequency has been chosen to be f_s = 20MHz. As in [8] the indices of the zero subcarriers within an OFDM symbol $\tilde{\mathbf{x}}$ are set to {0, 27, 28,...,37}. The optimum choice of the indices of the redundant subcarriers is given by {2, 6, 10, 14, 17, 21, 24, 26, 38, 40, 43, 47, 50, 54, 58, 62}. This choice, which can easily also be described by (1) with appropriately constructed matrices $\mathbf{B}$ and $\mathbf{P}$, minimizes the cost function $\operatorname{tr}\left(\mathbf{T}\mathbf{T}^H\right)$ discussed above. Fig. 2 shows

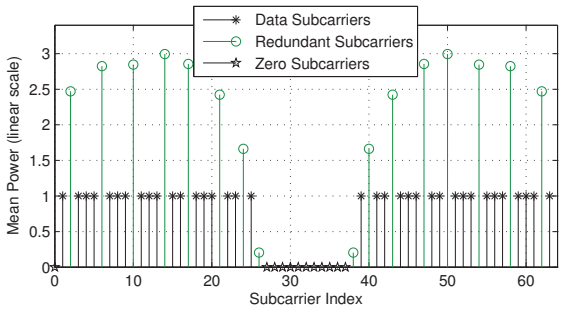

Fig. 2. Mean power of individual subcarrier symbols for the specified parameter setup.

the mean power values of all individual subcarrier symbols for the chosen parameter setup for the case the UW is the zero word $\mathbf{x}_u = \mathbf{0}$. The mean power for the data subcarrier symbols is $\sigma_d^2 = 1$, while the optimized mean power values of the redundant subcarrier symbols are the elements of the vector $\sigma_d^2\operatorname{diag}\left(\mathbf{T}\mathbf{T}^H\right)$ evaluated for the optimum permutation matrix $\mathbf{P}$.

In the following, we use the notation

$$\tilde{\mathbf{c}} = \mathbf{P}\begin{bmatrix}\tilde{\mathbf{d}}\\ \tilde{\mathbf{r}}\end{bmatrix} = \mathbf{P}\begin{bmatrix}\mathbf{I}\\ \mathbf{T}\end{bmatrix}\tilde{\mathbf{d}} = \mathbf{G}\tilde{\mathbf{d}}. \tag{7}$$

$\tilde{\mathbf{c}} = [\tilde{c}_0, \tilde{c}_1, ..., \tilde{c}_{N_d+N_r-1}]^T \in \mathbb{C}^{(N_d+N_r)\times 1}$ can be interpreted as a codeword of a complex number Reed Solomon code construction along the subcarriers. $\mathbf{G}$ represents the code generator matrix. Fig. 3 graphically illustrates the generation of a code word $\tilde{\mathbf{c}}$.

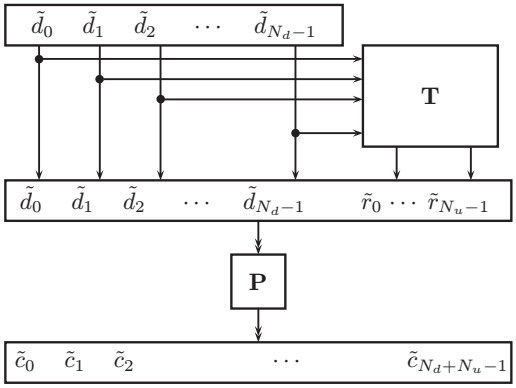

Fig. 3. Code word generator.

Since the code generator matrix $\mathbf{G}$ is known to the receiver, it can be exploited in the data estimation process. The utilization of this a-priori knowledge leads to a coding gain. Algebraic decoding of the described complex number RS code is extremely ill-conditioned, cf. [9]. In [1] we derived an LMMSE data estimator instead. We will only present the resulting equations here: Let $\tilde{\mathbf{y}} \in \mathbb{C}^{(N_d+N_r)\times 1}$ be the non-zero part of a received OFDM frequency domain symbol, $\tilde{\mathbf{H}} \in \mathbb{C}^{(N_d+N_r)\times(N_d+N_r)}$ be the diagonal channel matrix containing the sampled channel frequency response on its main diagonal, and $\tilde{\mathbf{x}}_u = \mathbf{F}_N \begin{bmatrix}\mathbf{0}^T & \mathbf{x}_u^T\end{bmatrix}^T$. Then the LMMSE data estimator is

$$\hat{\tilde{\mathbf{d}}} = \tilde{\mathbf{W}}\tilde{\mathbf{H}}^{-1}(\tilde{\mathbf{y}} - \tilde{\mathbf{H}}\mathbf{B}^T\tilde{\mathbf{x}}_u), \tag{8}$$

with the Wiener smoothing matrix

$$\tilde{\mathbf{W}} = \mathbf{G}^H\left(\mathbf{G}\mathbf{G}^H + \frac{N\sigma_n^2}{\sigma_d^2}(\tilde{\mathbf{H}}^H\tilde{\mathbf{H}})^{-1}\right)^{-1}. \tag{9}$$

We notice that the error $\tilde{\mathbf{e}} = \tilde{\mathbf{d}} - \hat{\tilde{\mathbf{d}}}$ has zero mean, and its covariance matrix is given by

$$\mathbf{C}_{\tilde{e}\tilde{e}} = \sigma_d^2\left(\mathbf{I} - \tilde{\mathbf{W}}\mathbf{G}\right). \tag{10}$$

For the case an additional outer channel code is applied, the main diagonal of $\mathbf{C}_{\tilde{e}\tilde{e}}$ containing the noise variances along the data subcarrier symbols can further be used in the channel decoding process.

III. UW Generation with Systematic Noise in the Guard Interval

With the introduction and optimization of the permutation matrix $\mathbf{P}$ we minimized the total energy of the redundant subcarrier symbols on average. Nevertheless, in our simulation setup the redundant energy is still in the same magnitude as that of the data symbols, cf. Fig 2. One way to further reduce the redundant energy is to allow for some systematic noise $\Delta\mathbf{x}_u$ in the UW. This can be incorporated in the first step of the UW generation process by replacing the zero UW in (2) by $\Delta\mathbf{x}_u$:

$$\begin{bmatrix}\mathbf{M}_{11} & \mathbf{M}_{12}\\ \mathbf{M}_{21} & \mathbf{M}_{22}\end{bmatrix}\begin{bmatrix}\tilde{\mathbf{d}}\\ \tilde{\mathbf{r}}\end{bmatrix} = \begin{bmatrix}\mathbf{x}_d\\ \Delta\mathbf{x}_u\end{bmatrix} \tag{11}$$

This leads to an underdetermined system of equations for $\tilde{\mathbf{r}}$ and $\Delta\mathbf{x}_u$ that can be written as

$$\begin{bmatrix}\mathbf{M}_{22} & -\mathbf{I}\end{bmatrix}\begin{bmatrix}\tilde{\mathbf{r}}\\ \Delta\mathbf{x}_u\end{bmatrix} = -\mathbf{M}_{21}\tilde{\mathbf{d}}. \tag{12}$$

We use the notation $\mathbf{A} = \begin{bmatrix}\mathbf{M}_{22} & -\mathbf{I}\end{bmatrix}, \mathbf{b} = -\mathbf{M}_{21}\tilde{\mathbf{d}}, \mathbf{z} = \begin{bmatrix}\tilde{\mathbf{r}}^T & \Delta\mathbf{x}_u^T\end{bmatrix}^T$, define a weighting matrix

$$\mathbf{W} = \mathrm{diag}\left\{\begin{bmatrix}\mathbf{w}_r\\ \mathbf{w}_u\end{bmatrix}\right\} \tag{13}$$

with the weighting vectors $\mathbf{w}_r$ and $\mathbf{w}_u$ consisting of non-negative elements, and suggest to find the solution of

$$\mathbf{A}\mathbf{z} = \mathbf{b} \tag{14}$$

that minimizes the cost function

$$g(\mathbf{z}) = \mathbf{z}^H\mathbf{W}\mathbf{z}. \tag{15}$$

In other words we aim to solve the following optimization problem:

$$\min\{\mathbf{z}^H\mathbf{W}\mathbf{z}\} \quad \text{s.t. } \mathbf{A}\mathbf{z} = \mathbf{b} \tag{16}$$

The solution of this optimization problem is

$$\mathbf{z} = \mathbf{W}^{-1}\mathbf{A}^H(\mathbf{A}\mathbf{W}^{-1}\mathbf{A}^H)^{-1}\mathbf{b}, \tag{17}$$

cf. [10]. With

$$\mathbf{T}' = -\begin{bmatrix}\mathbf{I} & \mathbf{0}\end{bmatrix}\mathbf{W}^{-1}\mathbf{A}^H(\mathbf{A}\mathbf{W}^{-1}\mathbf{A}^H)^{-1}\mathbf{M}_{21}, \tag{18}$$

the redundant subcarrier symbols can now be derived by

$$\tilde{\mathbf{r}} = \mathbf{T}'\tilde{\mathbf{d}}, \tag{19}$$

cf. (5). By replacing $\mathbf{G}$ with $\mathbf{G}' = \mathbf{P}\begin{bmatrix}\mathbf{I} & (\mathbf{T}')^T\end{bmatrix}^T$ the same formalism as in (7) also holds for the code word generation.

Note that we can now choose $N_r < N_u$, since additional degrees of freedom have been introduced by allowing for some systematic noise $\Delta\mathbf{x}_u$ in the UW. Consequently, the bandwidth efficiency can be increased. Clearly, the systematic noise in the UW

$$\Delta\mathbf{x}_u = -\begin{bmatrix}\mathbf{0} & \mathbf{I}\end{bmatrix}\mathbf{W}^{-1}\mathbf{A}^H(\mathbf{A}\mathbf{W}^{-1}\mathbf{A}^H)^{-1}\mathbf{M}_{21}\tilde{\mathbf{d}}, \tag{20}$$

which depends on the data vector $\tilde{\mathbf{d}}$, will be different from (OFDM) symbol to symbol. Like additive white Gaussian noise (AWGN) the systematic noise disturbs the cyclic property to some extent. We neglect the systematic noise in the receiver design and re-use the LMMSE data estimator by simply replacing $\mathbf{G}$ with $\mathbf{G}'$ in (9)-(10).

IV. Simulation results

To demonstrate the potential of the novel concept we compare it to the CP-OFDM based IEEE 802.11a standard, and to the original UW-OFDM setup used in [1] (as specified in Table I). The transceiver processing is as follows: The transmitter processing starts with (outer) channel coding, interleaving and QAM-mapping. We used the same outer convolutional encoder as defined in [8], and show results for (outer) coding rates $r = \frac{3}{4}$ and $r = \frac{1}{2}$, respectively. The interleaver in [8] has slightly been adapted to our specifications. Next the redundant subcarrier symbols are determined using (5) (for the original UW-OFDM concept) or (19) (for the novel concept). After assembling the OFDM symbol, cf. Fig. 3 and (1), the IFFT (inverse fast Fourier transform) is performed. Finally, the UW is added in the time domain. The receiver processing starts with an FFT, then the influence of the UW is subtracted, cf. (8), and the LMMSE data estimation is applied. Finally, demapping, deinterleaving and decoding is performed. For the soft decision Viterbi decoder the main diagonal of the matrix $\mathbf{C}_{\tilde{e}\tilde{e}}$ is exploited. In our approach the unique word shall take over the synchronization tasks which are performed with the help of the 4 pilot subcarriers in the reference system (802.11a). In order to make a fair comparison, the energy of the UW related to the total energy of a transmit symbol is set to 4/52, which exactly corresponds to the total energy of the 4 pilots related to the total energy of a transmit symbol in the IEEE standard. Note that the particular design of the UW has no impact on the BER behavior, cf [2]. In all simulations below we assumed perfect channel knowledge at the receiver.

Exemplarily we show simulation results for two different frequency selective indoor radio channel snapshots, both featuring an rms (root mean square) delay spread of 100ns. The frequency responses of the channel snapshots are shown in Fig. 4. Channel A features two spectral notches within the system's bandwidth, whereas channel B does not show deep fading holes.

For the novel concept we always used $\mathbf{w}_r = \mathbf{1}$, where $\mathbf{1}$ is a column vector with all entries being 1. For the elements of $\mathbf{w}_u$ we investigated two different approaches, namely a constant weighting vector with the elements $w_u[n] = c$, and a weighting vector defined by $w_u[n] = Ae^{n/\tau}$ for $n = 0, 1, ..., N_u - 1$. For a constant weighting vector all UW samples are treated equally, while in the second approach we try to force the systematic noise to tend to be larger in the beginning of $\Delta\mathbf{x}_u$, and to decrease along the UW. For the QPSK-mode the choice $c = 250$ showed promising results, however, the choice $w_u[n] = Ae^{n/\tau}$ with appropriately chosen parameters

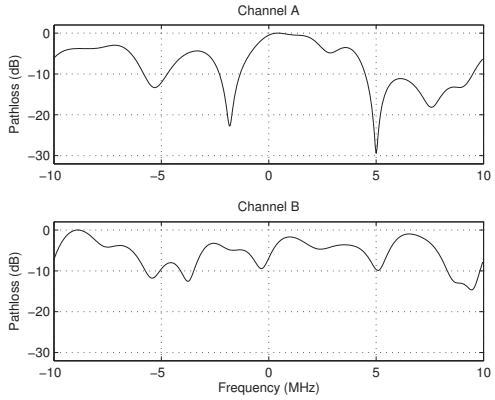

Fig. 4. Frequency responses of indoor multipath channel snapshots.

produced better results in most of the simulated scenarios. We show results for four different system setups:

- CP-OFDM reference system (IEEE 802.11a) with the parameters as in Table I.
- UW-OFDM (setup 1) with perfectly constructed UW, and with parameters as in Table I.
- UW-OFDM (setup 2) with systematic noise in the guard interval, and with parameters as in Table I. We chose $w_u[n] = Ae^{n/2}$ with $A = 0.5$ for QPSK/$r = \frac{1}{2}$, $A = 1$ for QPSK/$r = \frac{3}{4}$, $A = 2$ for 16QAM/$r = \frac{1}{2}$, and $A = 4$ for 16QAM/$r = \frac{3}{4}$. Note that a larger value for A forces the systematic noise to become smaller, and at the same time makes the energy of the redundant subcarrier symbols larger. The parameter choices above have been found empirically by comparing the BER behavior of the system for a large number of channel scenarios.
- UW-OFDM (setup 3). As stated earlier we can now choose $N_r < N_u$. In this setup we use $N_d = 40$ and $N_r = 12$. The indices of the redundant subcarriers are chosen to be {2, 6, 14, 18, 22, 26, 38, 42, 46, 50, 58, 62}. A and τ are the same as in setup 2.

Fig. 5 exemplarily shows the power distribution along the subcarrier symbols for $A = 0.5, \tau = 2$ for system setup 2. By

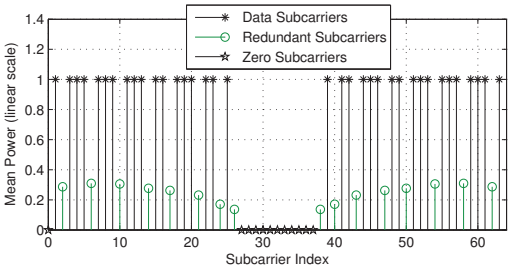

Fig. 5. Mean power of individual subcarrier symbols for UW-OFDM setup 2 ($A = 0.5, \tau = 2$).

comparing the results with those in Fig. 2 it can clearly be seen, that the energy contribution of the redundant subcarrier symbols has significantly been reduced.

Figures 6-8 show BER simulation results for the setups discussed above. Let us first concentrate on the QPSK-results

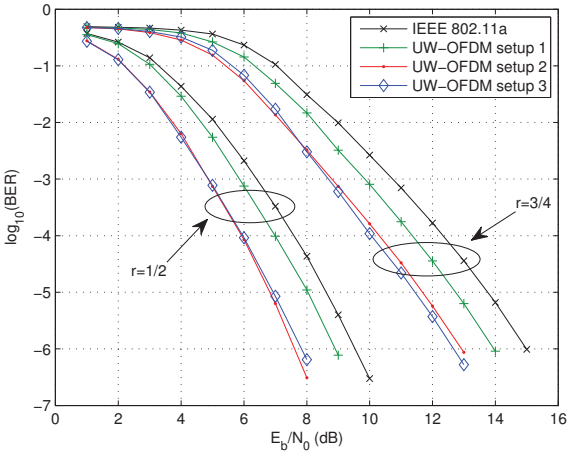

Fig. 6. BER comparison for channel A (QPSK).

for channel A, cf. Fig. 6. Despite the rather high redundant transmit energy UW-OFDM setup 1 already outperforms CP-OFDM by 1dB and 0.6dB for the outer coding rates $r = \frac{3}{4}$ and $r = \frac{1}{2}$, respectively (measured at a bit error ratio of 10^{-6}). This gain comes from the significant noise reduction (especially on highly attenuated subcarriers) achieved by the LMMSE data estimator compared to a simple channel inversion receiver, cf. [1]. A different view on this result is, that the code introduced in (7) together with the LMMSE 'decoder' achieves a coding gain over a simple channel inversion receiver (as it is used in CP-OFDM). For setup 2 the performance gain even increases to 2.1dB and 1.9dB, respectively. This can be explained by the reduction of the energy on the redundant subcarrier symbols. Setup 3 achieves similar gains while concurrently featuring an improved bandwidth efficiency. For

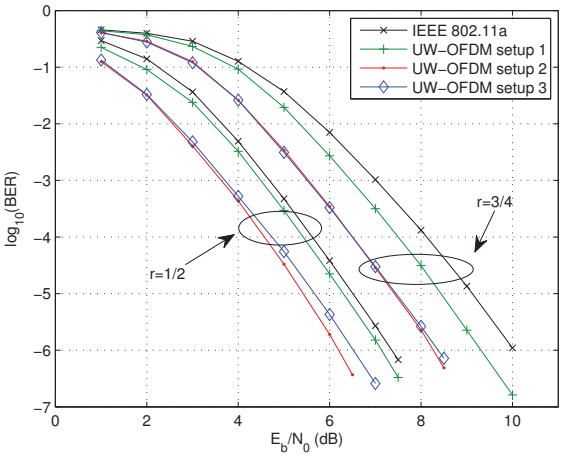

Fig. 7. BER comparison for channel B (QPSK).

channel B, cf. Fig. 7, the original UW-OFDM (setup 1) outperforms CP-OFDM by 0.7dB and 0.2dB for $r = \frac{3}{4}$ and $r = \frac{1}{2}$, respectively (again measured at a bit error ratio of 10^{-6}). Remarkable further performance improvements can again be observed for the novel concept (UW-OFDM setups 2 and 3). The gain over CP-OFDM increases to 1.8dB and 1.1dB, respectively, for setup 2, and to 1.7dB and 0.8dB, respectively, for setup 3. However, the performance gaps between UW-OFDM and CP-OFDM are smaller than for channel A. In fact it turns out that the coding gain achieved by the RS channel code inherently present in UW-OFDM is typically larger in channels featuring deep spectral notches, cf. also [1]. We notice that the disturbance of the cyclic property by the systematic noise in the UW is almost negligible for the investigated setups. In the interesting SNR-region AWGN dominates the systematic noise.

Fig. 8 shows the results for the 16QAM-mode in channel A. The achievable gains over the reference CP-OFDM system (e.g. 1.6dB and 1.5dB for UW-OFDM setup 2 for $r = \frac{3}{4}$ and $r = \frac{1}{2}$, respectively) and over the original UW-OFDM (setup 1) are again noticeable but smaller than for the QPSK-mode. At a given bit error ratio the AWGN noise in 16QAM-mode is smaller than for the corresponding QPSK-mode. Consequently the systematic noise produced by our approach becomes more dominant in the 16QAM-mode. We tried to counteract this fact by increasing A which results in a lower systematic noise, but unfortunately also in a higher redundant energy. Interestingly the BER curve for setup 3 and $r = \frac{1}{2}$ starts good but flattens for higher E_b/N_0 values, while setup 2 performs well for this case.

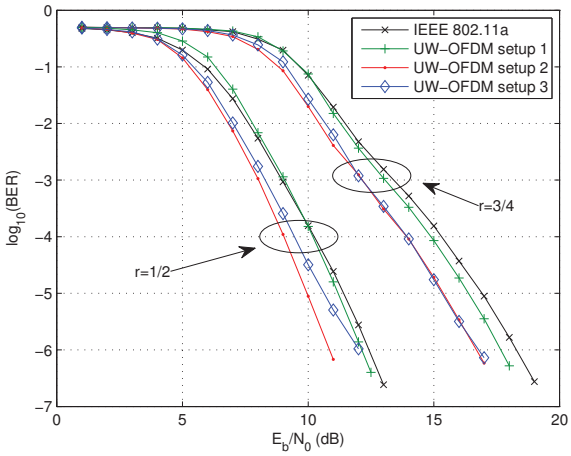

Fig. 8. BER comparison for channel A (16QAM).

V. Conclusion

In this work we expanded our recently introduced UW-OFDM concept by allowing some systematic noise in the unique word. The main effect is a significant decrease of the redundant energy. In spite of the reduced redundant energy the

inherently present RS code in combination with the LMMSE data estimator still shows strong performance, and the original UW-OFDM concept can clearly be outperformed in terms of the BER behavior.

REFERENCES

[1] M. Huemer, C. Hofbauer, J.B. Huber, "The Potential of Unique Words in OFDM", in the *Proceedings of the 15th International OFDM-Workshop*, Hamburg, Germany, pp. 140-144, September 2010.

[2] A. Onic, M. Huemer, "Direct versus Two-Step Approach for Unique Word Generation in UW-OFDM", in the *Proceedings of the 15th International OFDM-Workshop*, Hamburg, Germany, pp.145-149, September 2010.

[3] R. Cendrillon, M. Moonen, "Efficient equalizers for single and multi-carrier environments with known symbol padding", *IEEE International Symposium on Signal Processing and its Applications 2001 (ISSPA 2001)*, pp. 607-610, August 2001.

[4] M. Muck, M. de Courville, P. Duhamel, "A pseudorandom postfix OFDM modulator - semi-blind channel estimation and equalization", in the *IEEE Transactions on Signal Processing*, Vol. 54, Issue 3, pp 1005-1017, March 2006.

[5] D. Van Welden, H. Steendam, M. Moeneclaey, "Iterative DA/DD channel estimation for KSP-OFDM", *IEEE International Conference on Communications 2008 (ICC 2008)*, pp. 693-697, May 2008.

[6] S. Tang, F. Yang, K. Peng, C. Pan, K. Gong, Z. Yang, "Iterative channel estimation for block transmission with known symbol padding - a new look at TDS-OFDM", *IEEE Global Telecommunications Conference 2007 (GLOBECOM 2007)*, pp. 4269-4273, Nov. 2007.

[7] L. Jingyi, P. Joo, J. Ro, "The effect of filling Unique Words to guard interval for OFDM", Document IEEE C802.16a-02/87, IEEE 802.16 Broadband Wireless Access Working Group, September 2002.

[8] IEEE Std 802.11a-1999, Part 11: Wireless LAN Medium Access Control (MAC) and Physical Layer (PHY) specifications: High-Speed Physical Layer in the 5 GHz Band, 1999.

[9] W. Henkel, F. Hu, I. Kodrasi, "Inherent Time-Frequency Coding in OFDM and ISI Correction without a Cyclic Prefix", in the *Proceedings of the 14th International OFDM Workshop*, Hamburg, Germany, September 2009.

[10] S. Kay, *Fundamentals of Statistical Signal Processing: Estimation Theory*, Prentice Hall, Rhode Island 1993.